Estuarine, Coastal and Shelf Science 220 (2019) 1–12

Contents lists available at ScienceDirect

Estuarine, Coastal and Shelf Science

journal homepage: www.elsevier.com/locate/ecss

Slough evolution and legacy mercury remobilization induced by wetland restoration in South San Francisco Bay

Amy C. Foxgrover[a,*], Mark Marvin-DiPasquale[b], Bruce E. Jaffe[a], Theresa A. Fregoso[a]

[a] U. S. Geological Survey Pacific Coastal and Marine Science Center, Santa Cruz, CA, USA
[b] U. S. Geological Survey Water Resources, Earth System Processes Division, Menlo Park, CA, USA

ARTICLE INFO

Keywords:
Legacy contaminants
Mercury
Tidal slough
Sediment cores
Interferometric swath bathymetry
Bathymetric change
USA
California
South San Francisco Bay

ABSTRACT

Coastal wetlands have a long history of degradation and destruction due to human development. Now recognized as one of the most productive ecosystems in the world, substantial efforts are being made to restore this critical habitat. While wetland restoration efforts are generally viewed as beneficial in terms of providing wildlife habitat and flood control, they are often accompanied by dramatic physical and chemical changes that may result in unintended consequences, which are rarely studied. Alviso Slough, a tidal slough in South San Francisco Bay, California, is the site of an ongoing effort to restore former salt-production ponds to intertidal marsh habitat. Restoration is complicated by the fact that (1) the ponds undergoing restoration are severely subsided and (2) subsurface sediments within the slough and surrounding ponds are contaminated with legacy mercury deposits. Due to concerns regarding mercury remobilization, restoration has proceeded in a cautious, methodical manner. To assess the amount of legacy mercury remobilized since restoration began, we developed a technique of combining high-resolution, biannual measurements of bathymetric scour with mercury concentration measurements from sediment cores. We estimate that 52 kg (± 3) of mercury was remobilized in the 6 years since restoration began. Net bathymetric change analyses revealed seasonal trends of peak erosion during the winter months and little to no net change during summer months. Our analyses provide crucial insight on the spatial and temporal scales of geomorphic evolution within a tidal slough resulting from both natural (seasonal) variability and restoration actions. The technique presented here could be applied to other study sites and various sediment-associated contaminants of concern to aid in the design and management of restoration projects aiming to minimize negative impacts from legacy contaminants.

1. Introduction

Coastal wetlands are among the most productive ecosystems in the world (Barbier et al., 2011; Ramsar Convention, 2018). Wetlands serve as critical habitat for fish and wildlife (Goals Project, 1999), filter and improve water quality (Chapman and Wang, 2001; Day et al., 2012), buffer shorelines from the impacts of storms and sea-level rise (Kirwan and Megonigal, 2013; Rodríguez et al., 2017), sequester carbon dioxide from the atmosphere (Callaway et al., 2012; Nahlik and Fennessy, 2016) and provide valuable public recreation space. Unfortunately, coastal wetlands have been greatly impacted by human activities that resulted in either their destruction (through draining, diking, infilling) or degradation through land-use practices that have altered the flow of water and sediments to coastal estuaries (e.g., water diversions, dams, wastewater discharge, agriculture, mining operations, etc.). Located at the confluence of upland watersheds and the ocean, estuaries also serve as a receiving basin for anthropogenic contaminants flushed from the landscape. As a result, wetland restoration projects designed to restore these critical habitats face the additional challenge of mitigating negative impacts from sediment-associated legacy contaminants already in the system.

San Francisco Bay (SFB) is the site of the largest wetland restoration project on the west coast of the United States. The South Bay Salt Pond Restoration Project (SBSPRP) aims to restore 61 km^2 (15,100 acres) of former commercial salt-production ponds to a mix of intertidal habitats. However, restoration is complicated by mercury (Hg) contamination. Historic practices of gold-mining in the Sierra Nevada Mountains and Hg-mining in the California Coast Ranges delivered tens of thousands of tons of mercury from the upstream watersheds to North and South SFB, respectively (Alpers et al., 2005; Wright et al., 2014). Much of this Hg persists as a large pool of contaminated sediments stored within the Bay (Hornberger et al., 1999; Gehrke et al., 2011; Davis et al., 2012; Eagles-

* Corresponding author.
E-mail address: afoxgrover@usgs.gov (A.C. Foxgrover).

https://doi.org/10.1016/j.ecss.2019.02.033
Received 30 August 2018; Received in revised form 31 January 2019; Accepted 11 February 2019
Available online 18 February 2019
0272-7714/ Published by Elsevier Ltd.

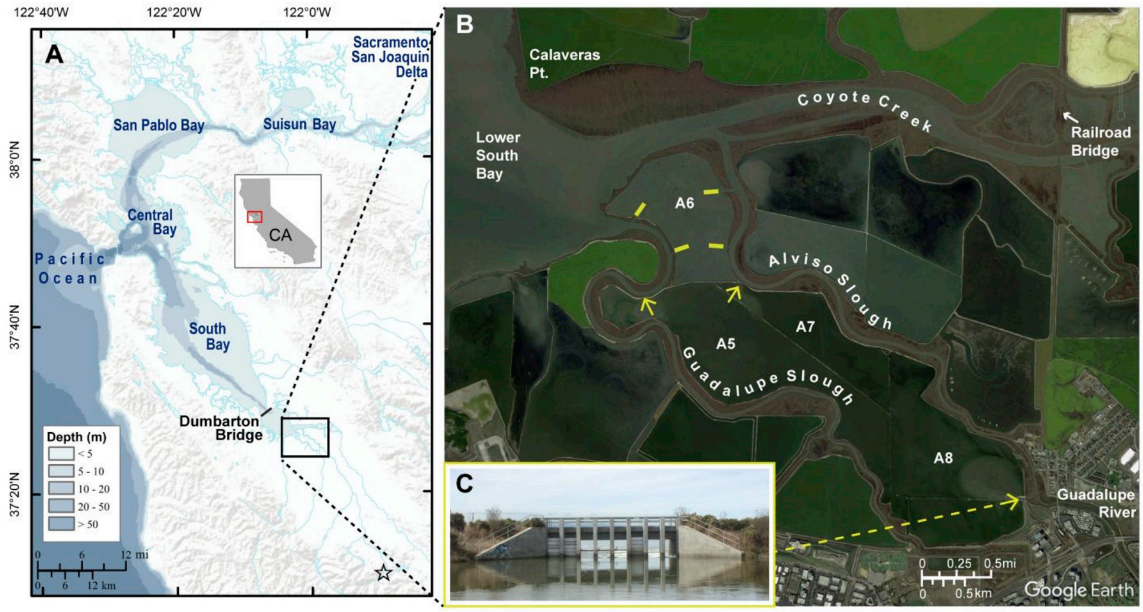

Fig. 1. Study Area. (A) San Francisco Bay, star denotes New Almaden mercury mines. (B) Lower South San Francisco Bay and Alviso Study area. Yellow rectangles indicate A6 breach locations and arrows are sites of flow control structures. (C) Pond A8 Tidal Control Structure (A8-TCS). (For interpretation of the references to color in this figure legend, the reader is referred to the Web version of this article.)

Smith et al., 2016). When buried beneath the surface of the Bay floor, the Hg-contaminated sediments are relatively harmless. However, once the previously sequestered Hg is liberated via sediment scour (i.e., remobilized) and exposed to active circulation in the contemporary aquatic environment, the Hg poses a serious risk to wildlife and ecosystem health (Grenier and Davis, 2010; Eagles-Smith et al., 2016). The concern is that, if sediment scour is increased as a result of restoration actions, and this legacy Hg is liberated, it has the potential for uptake through the aquatic food web (Marvin-DiPasquale and Cox, 2007; Davis et al., 2012), possibly harming the ecosystem and wildlife that the restoration project aims to protect. The ecological risks associated with Hg remobilization have been at the forefront of the SBSPRP's permitting, design, and implementation process (EDAW et al., 2007; SBSPRP, 2018).

The primary objective of this study was to quantify the amount of Total Hg (THg) remobilized within Alviso Slough, a tidal slough in South San Francisco Bay (SSFB), as wetland restoration progressed. We developed a new technique of combining biannual measurements of slough scour with THg concentration data from sediment cores to estimate THg remobilization within the slough. In doing so, we have not only quantified THg remobilization, but also produced a remarkable series of 13 high-resolution bathymetric surveys over the course of 6 years. This is the only dataset we are aware of that captures the changes in morphology of a tidal slough with this level of detail. This series of surveys offers an unprecedented view of the geomorphic evolution of a mesotidal slough in response to both natural, seasonal variability and changes in hydrodynamics resulting from restoration actions. This paper details the technique we developed for estimating THg remobilization from subsurface sediments as well as changes in slough bathymetry through time. Combined, these datasets assess the impact of both seasonal variability in natural forcings and restoration-induced modifications of flow to provide insight on the spatial extent, rate, and magnitude of morphologic change and associated mercury remobilization.

2. Study area

2.1. Regional setting

San Francisco Bay is the largest estuary on the west coast of the United States. Fresh water enters the estuary primarily through the Sacramento–San Joaquin River Delta, a drainage basin that covers ~40% of the state of California, and mixes with saline waters entering from the Pacific Ocean beneath the Golden Gate Bridge (Conomos et al., 1985). Tides are mixed semi-diurnal with a range that increases towards the south reaching 2.6 m at the Dumbarton Bridge (Fig. 1; NOAA, 2018). Lower SSFB, south of the Dumbarton Bridge, is extremely shallow (average depth of < 2 m at mean tide level), and intertidal flats cover over 70% of the surface area (Jaffe and Foxgrover, 2006). The surface sediments are composed primarily of silt and clay, with a mean grain size of 15 μm (Barnard et al., 2013).

San Francisco Bay has a Mediterranean climate with $> 95\%$ of the annual average precipitation delivered via episodic winter storms between October 1st and April 30th of each Water Year (WY spans October 1 –September 30 for any given year; McKee et al., 2013). The spring and summer months are marked by little precipitation and sea breezes, typically from the west or northwest (Conomos et al., 1985). Annual peak suspended sediment concentrations occur during the springtime at both the Dumbarton Bridge, 400–1200 mg/L (Shellenbarger et al., 2013) and within Alviso Slough, > 1500 mg/L (Shellenbarger et al., 2015). The two main tributaries to lower SSFB are Coyote Creek, which enters from the east and the Guadalupe River, which feeds into Alviso Slough.

2.2. Mercury in South San Francisco Bay

Hg contamination is a concern throughout the entire SFB estuary due to a combination of natural and anthropogenic sources (Gehrke et al., 2011; Davis et al., 2012; Eagles-Smith et al., 2016). Hg contamination is of particular concern in SSFB because the largest historical Hg mining district in North America, New Almaden, is located 30 km upstream and feeds into its waters (Cargill et al., 1980; Gehrke et al., 2011; McKee et al., 2017). Over 37 million kg of Hg was mined from the New Almaden mine between 1845 and 1975 during which mining waste and processed ore were deposited on the surrounding lands and creeks (Cargill et al., 1980). Over time, mining waste was transported downstream to the Guadalupe River, which feeds into lower SSFB. Although decommissioned in the 1970s, the legacy of the mining era is still apparent in elevated Hg concentrations in sediments throughout the watershed drainage to the Bay (Guadalupe River and upstream reservoirs; McKee et al. (2017)), the length of Alviso Slough

(Marvin-DiPasquale and Cox, 2007), within the surrounding ponds and marsh (Conaway et al., 2004; Miles and Ricca, 2010), and within the resident birds and fish (Schwarzbach et al., 2006; Ackerman et al., 2014; Eagles-Smith and Ackerman, 2014).

2.3. Alviso Slough and salt ponds

Alviso Slough is a region that has undergone extensive landscape modifications that have altered natural hydrologic flows including the construction of levees, commercial salt ponds, and upstream reservoirs as well as channel rerouting and dredging. Historically, Guadalupe River flowed directly to Guadalupe Slough rather than Alviso Slough (see historical maps in SFEI (2018)). In the mid-to-late 1800s a junction was formed connecting the two sloughs, and in the early 1900s when levees were constructed for salt evaporation ponds, the Guadalupe River was disconnected from Guadalupe Slough and has since drained directly into Alviso Slough. Since the salt pond levees were constructed in the early-to-mid 1900s, this region has subsided > 1 m as a result of excess groundwater withdrawal in the greater Santa Clara Valley (Poland and Ireland, 1988; Ingebritsen and Jones, 1999; Watson, 2004). Subsidence was largely halted by the 1970s, yet the interior of the ponds and the surrounding communities remain at elevations below mean tide level.

Our focus here is Alviso Slough itself, and the ponds to the west undergoing restoration. Alviso Slough is ~100 m wide where it meets Coyote Creek and tappers up slough to a width of 30 m or less near Pond A8 (Fig. 1). The slough is lined by marsh habitat, predominantly pickleweed and cordgrass in the lower slough and bulrush and cattails in the mid to upper slough (Fulfrost et al., 2012), which provides a buffer between the slough and the earthen levees surrounding the adjacent historic salt production ponds. Waters flow throughout the up-slough ponds (A5, A7, and A8) through a series of internal levee breaches. This larger combined complex (hereafter Pond A8 complex) covers 6.2 km^2 and is separated from the smaller (1.5 km^2) down-slough Pond A6 by an intact levee. Mean pre-restoration depths of 1.8 and 2.4 m below mean higher high water (MHHW) within Ponds A6 and A8, respectively (Foxgrover et al., 2007a,b; Athearn et al., 2010), translate to sediments voids on the order of $2.7 \times 10^6\ m^3$ and $14.6 \times 10^6\ m^3$. Combined, over $17 \times 10^6\ m^3$ of sediment is needed to fill the ponds to MHHW to sustain tidal marsh habitats and $7 \times 10^6\ m^3$ to reach the elevation of mean tide level where plants can begin to colonize. Opening these subsided ponds to tidal action has been projected to more than double the tidal prism of Alviso Slough (Achete, 2016).

2.4. Restoration design

Closest to the Bay, where Hg contamination is lower, a levee/dike breach style restoration (Pethick, 1996; Williams and Orr, 2002) was initiated in December of 2010. The levee surrounding Pond A6 was breached in four locations (two along Guadalupe Slough and two along Alviso Slough; Fig. 1) to allow the pond to naturally fill with sediment delivered via tidal flux. Just up slough from the breaches there are two pairs of 1.2-m-wide culverts modifying flow into or out of the larger Pond A8 complex through Ponds A5 and A7. Due to legacy Hg concerns associated with restoration of the larger Pond A8 complex, a dike breach approach was impermissible. Rather, a tidal control structure (A8-TCS) was constructed in the far southeastern corner of Pond A8, connecting the larger A8 pond complex to upper Alviso Slough (Fig. 1). The concrete structure is approximately 12 m wide and consists of 8 openings, each outfitted with a 1.5-m-wide gate that can be opened or closed independently to control water flow (Fig. 1c). A single gate was first opened for 6 months, June–December of 2011, and then closed over the winter months to prevent juvenile salmonids from getting trapped inside the ponds. Three gates were opened from June–December of 2012 and again in 2013. In March of 2014, three gates were once again opened, but rather than closing them during the winter, they remained open from that point forward, while the number of opened gates increased over the subsequent 3-year period. In September 2014, five gates were opened, and in June 2017 all eight gates were opened, and remain open as of 2018. The timing and extent of gate operations were determined in part based upon the results of the research presented here, in combination with numerous studies analyzing the physical and biological impacts of restoration (SBSPRP, 2018).

Alviso Slough provided a unique case study on the geomorphic evolution of a slough in response to a large increase in tidal prism resulting from two separate restoration actions: (1) open breaches that allowed the sudden introduction of tidal water to a smaller pond (Pond A6) in the lower slough and (2) a tidal control structure (TCS) in the upper slough and the gradual, controlled introduction of tidal waters to a larger (Pond A8) complex. As levees surrounding the subsided ponds are breached and the tidal prism enlarged; higher velocity tidal flows are anticipated to increase sediment scour within Alviso Slough. If restoration was shown to exacerbate Hg contamination within Alviso Slough, with the potential for long-term environmental impacts, the A8-TCS gates would be closed and tidal exchange halted (EDAW et al., 2007).

3. Methods

3.1. Bathymetric surveys

Tidal sloughs are a challenging environment in which to conduct bathymetric surveys. Typically, bathymetric change analyses in tidal sloughs or riverine environments are performed by transects with either single-beam bathymetry, lead line, or walking surveys performed at fixed intervals along the length of the study area, providing a cross-sectional view at specific locations, but no information on what occurred between transects. To obtain full coverage of Alviso Slough, a 234 kHz SWATHplus (aka BATHYSWATH) interferometric sidescan sonar system was pole-mounted to the U.S. Geological Survey (USGS) research vessel, *R/V Parke Snavely* (Foxgrover et al., 2018). The SWATHplus is optimized for collecting high-resolution bathymetry in shallow conditions, has a beam width greater than 12 times the water depth, and was able to map the entire slough in just two passes up and down the slough. The output is a continuous, 1-m horizontal resolution survey with an average density of 20 soundings per square meter.

The baseline, pre-restoration bathymetric survey in 2010 and all subsequent surveys were conducted following the procedures outlined in Foxgrover et al. (2018). During the fall of 2011 we began collecting bathymetric surveys on a biannual basis, spring and fall, to measure bathymetric change as restoration progressed. Spring (either March or April) and fall (either October or November) were targeted as our survey months to best capture seasonal fluctuations in regional sediment flux (Shellenbarger et al., 2013). We mapped the bathymetry of Alviso Slough (area of $\sim 250 \times 10^3\ m^2$) every spring and fall between October 2011 and March 2017, with the exception of spring 2014. All 13 of the bathymetric surveys (available from Foxgrover et al., 2018) were collected using the same methodology and referenced to the same datums so that they could be directly compared to one another for analyzing volumes and patterns of morphologic change through time. Bathymetric change was calculated by differencing pairs of bathymetric surveys.

There are two types of error associated with bathymetric surveys, bias and random error. Bias can enter through differences in horizontal or vertical datums (reference points), thereby introducing false, systematic offsets between surveys. Random error, on the other hand, is randomly distributed in space, has a mean of zero, and is generally associated with sounding inaccuracies or noise. Although each individual sounding contains some error, the large number of soundings both above and below a surface (average point density of $20/m^2$) will cancel out, resulting in a true average depth. In comparing bathymetry

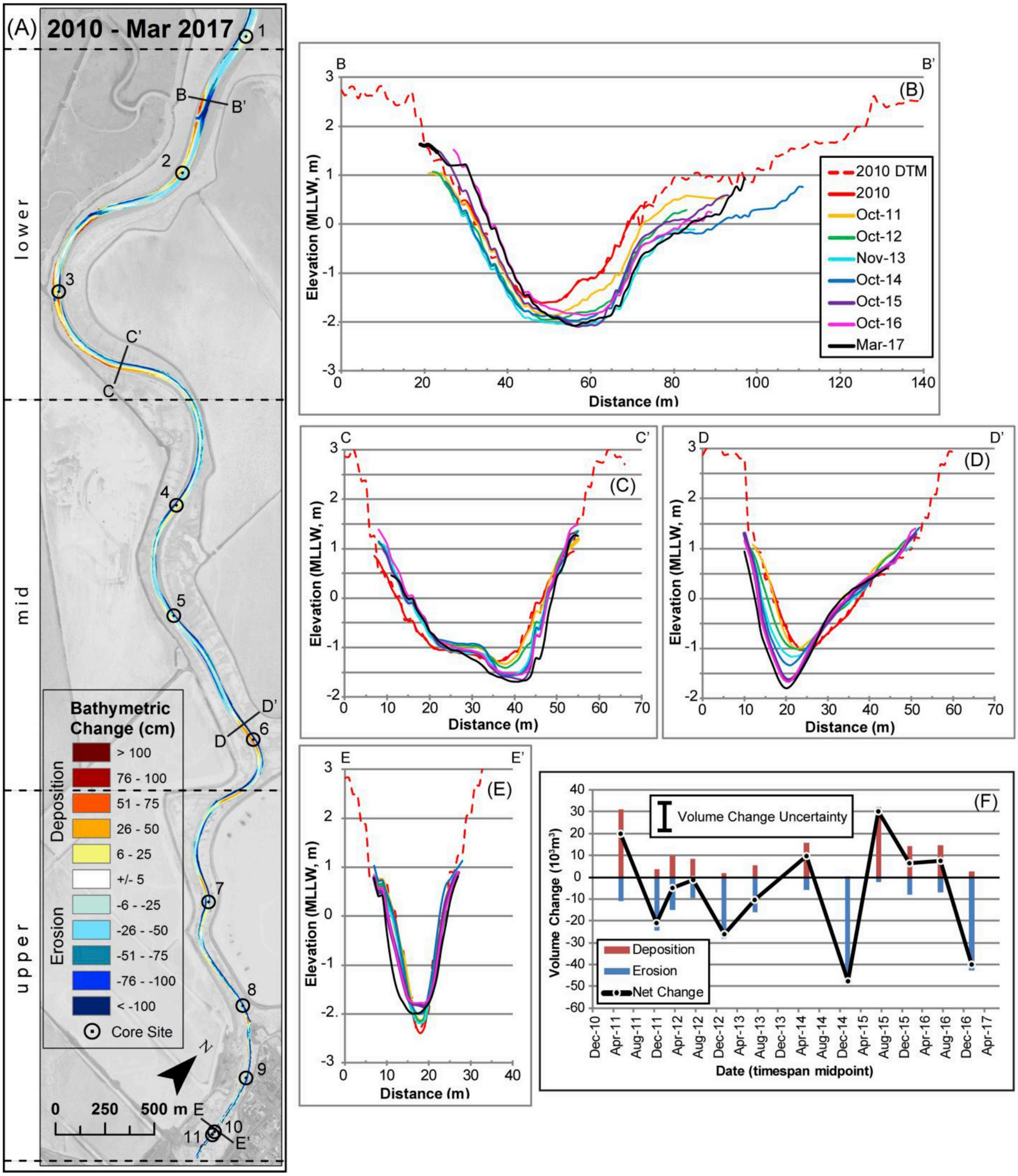

Fig. 2. A: Net bathymetric change from December 2010–March 2017. Location of sediment cores 1–11, cross-section profiles, and three slough reaches shown for reference. B–E: Slough cross-section profiles. 2010 digital terrain model (DTM) of 2010 bathymetry merged with aerial topographic lidar displayed to provide context on the upper portion of the banks not captured by bathymetric surveys. F: Volumes of gross erosion (blue), gross deposition (red), and net bathymetric change (black line) over the duration of our study. (For interpretation of the references to color in this figure legend, the reader is referred to the Web version of this article.)

from two time periods, random error cancels out whereas systematic bias will not. We assessed bias by comparing repeat surveys of the slough collected within days of one another. The mean difference in areas of overlap from five separate repeat surveys (spanning November 2013–March 2017) represents the bias between individual surveys (range of 1–5 cm, mean = 2 cm). Volume change uncertainty was approximated by adding the mean bias for each survey (2 cm), in quadrature and multiplying the result (3 cm) by the surface area of the bathymetric change grid.

For the purposes of our analyses, we divided the slough into three reaches of comparable slough lengths; lower (0.2–2.7 km from the mouth), mid (2.7–5.0 km from the mouth), and upper (5.0–7.1 km from the mouth; Fig. 2). The difference in cross-sectional areas between these reaches is noteworthy. While the greatest volume change often occurred within the lower slough, where the slough is widest, when normalized by area (i.e., centimeter of vertical change per square meter of surface area) the mid and upper slough can exceed the area-normalized change of the lower slough. Graphs of change through time are thus normalized by surface area so the results are directly comparable across all three slough reaches. For simplicity, when referring to changes that occurred in the late fall and winter, we use the end year naming convention, e.g., change from October 2014–April 2015 is simply ‘2015 winter’.

3.2. Sediment core collection and Hg analyses

A total of 12 sediment cores were collected along the center of Alviso Slough over three separate coring campaigns during September 2006 (5 cores), May 2012 (4 cores), and January 2016 (3 cores). The sampling locations of Cores 1–11 are displayed on Fig. 2. Core 12 (not shown) was collected outside of the bathymetric survey extent, ~500 m up slough of Core 11. All of the 2006 core analytical results and methodological details associated with field sampling, core logging, and laboratory analysis of Hg and non-Hg species have been previously published (Marvin-DiPasquale and Cox, 2007). The same field and laboratory methods were used for the 2012 and 2016 cores, and the analytical results are available on-line (Marvin-DiPasquale et al., 2018). Core lengths ranged from 79 cm to 231 cm (mean = 189 cm, median = 198 cm). Sub-sampling intervals typically ranged from 10 to 30 cm and were determined based on visual changes in stratigraphic features (color, apparent grain size) of the longitudinally split cores and non-destructive scans of sediment bulk density and magnetic susceptibility (Marvin-DiPasquale and Cox, 2007). However, for the purposes of modeling sediment Hg mobilization (this study), THg concentrations (ng/g dry weight) were converted to regularly spaced 10-cm intervals by linear interpolation and then transformed to (ng/cm^3) using coincident measurements of sediment bulk density.

3.3. Hg remobilization calculations

While there is a mobile/active layer of Hg-contaminated near-surface sediments exposed to the aquatic environment through shallow tidal mixing or bioturbation, that is not our primary focus here. Our main focus is the sediment-associated Hg deposits buried beneath the Bay floor of Alviso Slough, originating primarily from runoff of the now decommissioned New Almaden Hg mine (hereafter legacy Hg). In this dynamic estuarine environment, sediments are often reworked, with periods of erosion followed by deposition and vice versa. However, in this study we are most concerned with the initial exposure of long buried, Hg-contaminated bed sediments to Bay waters. For example, for a given location the deepest point of erosion may have occurred during April 2015, but was then covered by newly deposited sediments in the weeks or months following. Regardless, that April 2015 depth is what we used for our Hg remobilization calculation for this location. Whether or not sediments were redeposited in that same location later was not accounted for in our calculations since the origin of those sediments would be unknown and our primary concern was the initial exposure of the ecosystem to remobilized legacy Hg. For a number of reasons (detailed in Section 5.1) this approach may be considered a conservative estimate of THg available to the ecosystem.

The series of 13 seasonal bathymetric surveys were imported into ArcGIS software for bathymetric change analyses. The maximum depth of scour over the entire time series was extracted using the Cell Statistics Tool in ArcGIS to select the deepest measurement for each individual 1 × 1 m grid cell over the entire slough. The resulting raster surface represents the maximum depth measured for each individual grid cell within Alviso Slough throughout the 12 seasonal surveys collected between October 2011 and March 2017. The maximum depth surface was then differenced from the 2010 baseline survey to generate a surface of the maximum amount of scour since restoration began.

Data from 12 sediment cores were used to capture the variability of THg concentration with depth beneath the slough floor and also with distance along the slough (locations shown in Fig. 2). Although the sediment cores were collected over three separate coring campaigns (2006, 2012, and 2016), our scour calculations are all relative to the 2010 pre-restoration baseline bathymetry. To account for this difference in time, within our model we adjusted the vertical position of the sediment cores to the same reference plane as the 2010 baseline bathymetry. The amount of bathymetric change that occurred between 2010 and the core collection date was approximated using bathymetric surveys most recent to core collection. A single-beam survey from April 2005 (Foxgrover et al., 2007b) and our April 2012 and October 2015 SWATHplus surveys were used for reference. The average amount of sediment erosion or deposition that occurred within a 3-m radius of the core collection site between the approximate time of collection and 2010 was used to shift the cores vertically to match the 2010 reference plane. For the two cores that did not extend to 2 m depth (Cores 11 and 12), or for very localized erosional hotspots where sediment scour exceeded 2 m (< 0.1% of the study area), the THg concentration from the deepest measured interval was applied to underlying sediments.

Once all of the cores were shifted to the 2010 vertical reference plane, 10-cm-thick horizons of THg concentration were linearly interpolated between core sites along the length of the slough and down to a depth of 2 m below the 2010 baseline elevation surface. In all, a total of 20 data layers captured THg concentration variation, one for each 10-cm-thick sediment horizon along the length of the slough. For each survey time step, the maximum depth of scour was calculated on a cell-by-cell basis for the entire slough. The depth of scour was then converted to a volume of sediment eroded (cm^3) for each 10-cm horizon and multiplied by the THg concentration (in ng/cm^3) for that specific slough location and depth. The values were summed by survey time step to calculate mass of THg remobilized as a result of sediment scour within the slough since December 2010.

The largest uncertainty in our remobilization calculation is attributed to the high spatial variability of THg concentration in slough sediments. Admittedly, a linear interpolation based upon 12 cores is a simplified representation of true spatial variability over the entire slough. To estimate uncertainty we applied two additional techniques for approximating THg concentration within the slough: (1) using a single, depth-averaged THg concentration for each slough reach derived from average core concentrations, and (2) using average THg concentration per slough reach for each 10-cm-thick horizon. These two techniques generated remobilization numbers within ± 5% of the more sophisticated interpolation method.

4. Results

4.1. Slough morphology and bathymetric change

Patterns of morphologic change varied spatially along the length of the slough. Sections of the slough channel migrated laterally (one side deposited and the other eroded), widened (both banks eroded while the thalweg remained stable), deepened, or shoaled (Fig. 2). As of March 2017 approximately 75% of Alviso Slough was deeper than in the pre-restoration 2010 survey (average erosion = 42 cm). In terms of total survey area, 51% eroded < 0.5 m, 16% from 0.5 to 1 m, 5% from 1 to 1.5 m, and 1% from 1.5 to 2 m. Scour > 2 m (< 0.1% of the area) was confined to localized hotspots immediately adjacent to breaches, culverts, or the tidal control structure at Pond A8 (A8-TCS). The remaining 25% of the slough was depositional (average = 21 cm).

In addition to spatial variability, sedimentation patterns also varied through time (Fig. 2f). In the 6 years following the A6 breaches (December 2010–October 2016) there was a net erosion of 26×10^3 m^3 (± 7). With the winter of 2017 included (December 2010–March 2017), net erosion increased to 58×10^3 m^3 (± 7). This highlights the point that due to seasonal and inter-annual variability, net change

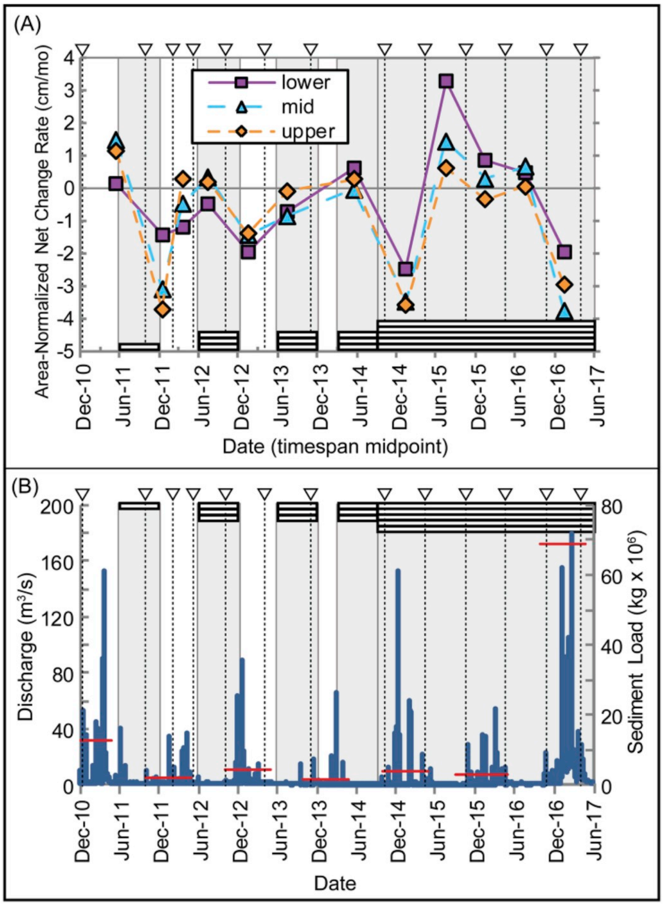

Fig. 3. A: Area-normalized net change rate (cm/mo) per slough segment. Vertical dashed lines represent bathymetric survey dates, the gray shading and rectangles across the X-axis are A8-TCS gate openings (1 box per gate). B: 15-min Guadalupe River discharge (blue lines) and cumulative suspended sediment loads per wet season (horizontal red lines) (USGS station 11169025). (For interpretation of the references to color in this figure legend, the reader is referred to the Web version of this article.)

volumes vary significantly based upon the time period over which they were calculated. Therefore, we have emphasized comparable time steps and seasons when interpreting change results.

Within each year there was significant seasonal variability and a general pattern of higher volumes of net erosion during the winter months (average erosion of $24 \times 10^3\,m^3$, max of $48 \times 10^3\,m^3$) and either decreased amounts of erosion or net sedimentation over the spring and summer months (average deposition of $7 \times 10^3\,m^3$, max of $30 \times 10^3\,m^3$; Fig. 2f). Out of the five winter seasons surveyed, all except the 2016 winter had a net erosion of sediment with peak area-normalized net-erosion rates of 3 cm/mo for the entire slough (Fig. 3). Net change over the four summer periods generally fluctuated between slightly erosional to slightly depositional. The highest rate of area-normalized net deposition recorded in our study, an average of 2.1 cm/mo over the entire slough, occurred during the summer of 2015 (Fig. 3).

Throughout the duration of our study, the hydrodynamics within the slough were influenced by restoration actions (A6 breaches and A8-TCS operations) as well as natural variability in freshwater delivery from the Guadalupe River (Fig. 3). Guadalupe River discharge was measured at USGS gaging station 11169025, approximately 8 km upstream of the A8-TCS (USGS, 2018a). Much of our study period, Water Years (WY) 2012–2015, coincided with a severe drought in California. There was near-average precipitation in WY 2016 and record precipitation in WY 2017 (McKee et al., 2017; East et al., 2018; Swain et al., 2018). On February 21, 2017, the Guadalupe River gage recorded the highest maximum peak discharge since 1998. Based upon 87 years of flow measurements (combined records of 2 nearby gages (USGS, 2018a; USGS, 2018b)), the February 21st peak of $180\,m^3/s$ had an estimated recurrence interval of 5–10 years. Perhaps what is more impressive is that during WY 2017 six flow events exceeded $77\,m^3/s$, the equivalent of a 2-year flood event. In other words, there is a 50% chance of a flow of this magnitude happening in any given year, and there were 6 in early 2017. The high flows of WY 2017 were also associated with high sediment loads. Nearly 75,000 tons ($\sim 68 \times 10^6$ kg) of sediment passed the Guadalupe River gage from October 2016–March 2017 (Fig. 3), nearly 25 times the average winter loads of the preceding 5 years (USGS, 2018a).

Over the course of our study there were three comparable peaks of net erosion (Fig. 3). During the first erosional peak, in the winter of 2012, the rate of area-normalized net change was highest in the upper slough, -3.7 cm/mo, and decreased to -1.4 cm/mo in the lower slough. The early winter of 2012 was a period of relatively low discharge and only one of the A8-TCS gates had been opened for 6 months (Fig. 3). The second erosional peak was not until the winter of 2015 and encompassed a large discharge event in December (peak of $150\,m^3/s$). Furthermore, it was the first time the A8-TCS gates were left open all winter and the A8-TCS opening was expanded from 3 to 5 gates at the end of September 2014. During the third erosional peak in the winter of 2017, the A8-TCS had remained open at 5 gates for over 2 years, Guadalupe River had record-high discharges (detailed above) and the mid slough had the highest net erosion rate, -3.7 cm/mo (Fig. 3).

In the first year following the breaches of the A6 levees, the amount of erosion immediately adjacent to the breaches was countered by a nearly equivalent amount of sediment deposition just up slough, resulting in a slight net deposition of sediment in the lower slough over the first year. Over the subsequent 2 years (October 2011–November 2013), the lower slough experienced net erosion (Fig. 4). Beginning in November 2013 this trend reversed and the lower slough became net depositional. With the exception of the 2015 winter, there was a cumulative net deposition of sediment in the lower reach from November 2013 through October 2016. During both the winters of 2015 and 2017 all reaches were net erosional; however, the lowest rates of erosion remained in this lower reach (Fig. 3).

Greater context for the changes within Alviso Slough were obtained through comparisons of geomorphic change within Pond A6 and beyond the mouth of Alviso in lower SSFB. An average annual sediment accumulation rate of 20 cm/yr was measured at 10 sediment pins distributed throughout Pond A6 in the 28 months following the levee breaches (Callaway et al., 2013). The average accumulation of 47 cm over the surface area of Pond A6 equates to a deposition of over

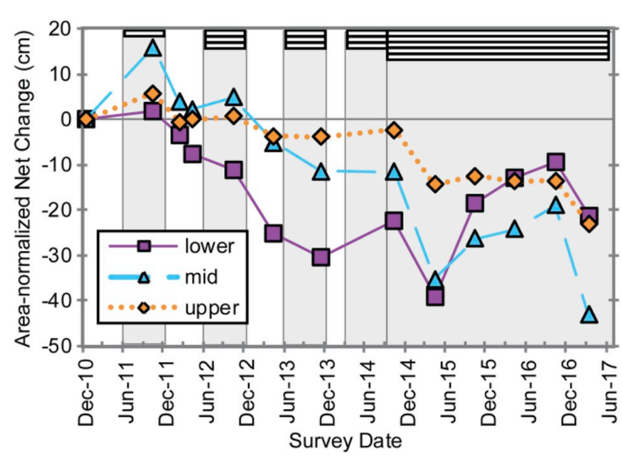

Fig. 4. Cumulative area-normalized net change (cm) per slough segment. Negative changes represent erosion and positive deposition. Gray shading and rectangles across the X-axis are A8-TCS gate openings (1 box per gate).

625×10^3 m^3 of sediment (Callaway et al., 2013) or approximately 7 times the cumulative gross erosion from Alviso Slough over the same timeframe (88×10^3 m^3 during December 2010–April 2013). Since the volume of sediment deposited within Pond A6 exceeded the erosion within Alviso Slough, sediments must have been transported from beyond the vicinity immediately adjacent to Pond A6, a conclusion which is further supported by our larger bathymetric change maps (Figs. S1 and S2). Although the scope of the immediate study is focused on Alviso Slough, our bathymetric surveys also covered the surrounding area within lower SSFB, along Coyote Creek from east of Calaveras Point to the railroad bridge, along the lower 3.7 km of Guadalupe Slough, and when tides permitted, the adjacent tidal flats. The pattern of increased erosion during the winter and decreased erosion/net deposition over the summer documented within Alviso Slough also existed throughout our larger study area (Figs. S1 and S2).

4.2. Mercury remobilization

To assess the remobilization of Hg deposits from within Alviso Slough's subsurface sediments, we focused our analyses on the timing and magnitude of the maximum depth of scour (Fig. 5), the deepest point of erosion measured over the duration of our surveys, and the associated volume of sediment scoured from the slough. Once the subsurface Hg deposits have been remobilized and exposed to surface water, a number of things can happen, including: a) inorganic Hg(II) previously associated with solid-phased reduced mineral species (e.g. FeS, FeS_2) can become more readily available for biological uptake as those solid-phase substrates become oxidized; b) Hg(II) can become available for microbial conversion to methylmercury; c) particulate associated Hg(II) and methylmercury can be transported as newly suspended material throughout the system (up or down slough, into ponds, or into fringing wetlands) (Marvin-DiPasquale and Cox, 2007). For much of the lower slough the maximum scour depth was reached by April 2015, whereas the deepest points measured in the mid and upper slough were primarily from the final survey in March 2017 (Fig. 5b).

Sediment cores revealed a high degree of spatial variability, both horizontally and vertically, in THg concentration throughout the slough. THg concentration ranged from 0.04 to 10.4 μg/g (mean = 1.0, median = 0.8). The median of 0.8 μg/g is comparable to pre-restoration surface sediment samples collected within the Alviso ponds, 0.7 μg/g (Miles and Ricca, 2010), which is the concentration shown to frequently cause adverse biological effects in benthic fauna (Long et al., 1995). Concentrations in the surface interval of the cores tended to be lower than in subsurface sediments (median of 0.6 μg/g), but still elevated compared to samples from throughout SFB; from deep cores (range of 6 surface samples = 0.3–0.4 μg/g; Hornberger et al., 1999), intertidal and wetland locations (N = 29, median = 0.3 μg/g; Gehrke et al., 2011), and subtidal samples (N = 51, median = 0.2 μg/g; Conaway et al., 2003).

Although the sediment cores revealed a general pattern of higher THg concentration in deeper sediments in the mid to upper slough, there was not a consistent trend of increased Hg with core depth or distance up slough (Fig. 6). Given the complex depositional history, environmental setting, and number of hydrologic modifications to the slough over the past 150 years, this is not surprising. There is, however, a general pattern of increased concentrations at depths > 30 cm, with the mid and upper slough cores having the highest overall concentrations, and the 3 highest peak measurements (all > 4000 ng/cm^3) found in the upper slough (Fig. 6).

During the first 3 years of the restoration project, rates of THg remobilization increased modestly in the winter months coincident with increased rates of erosion (Fig. 7a), but generally averaged about 3 mg/mo/m^2 and were comparable across all slough reaches (Fig. 7b). However, in the winters of 2015 and 2017 larger spikes of THg remobilization (9–16 mg/mo/m^2) occurred in the mid and upper sloughs (Fig. 7b). The cumulative volume of sediment erosion and the THg

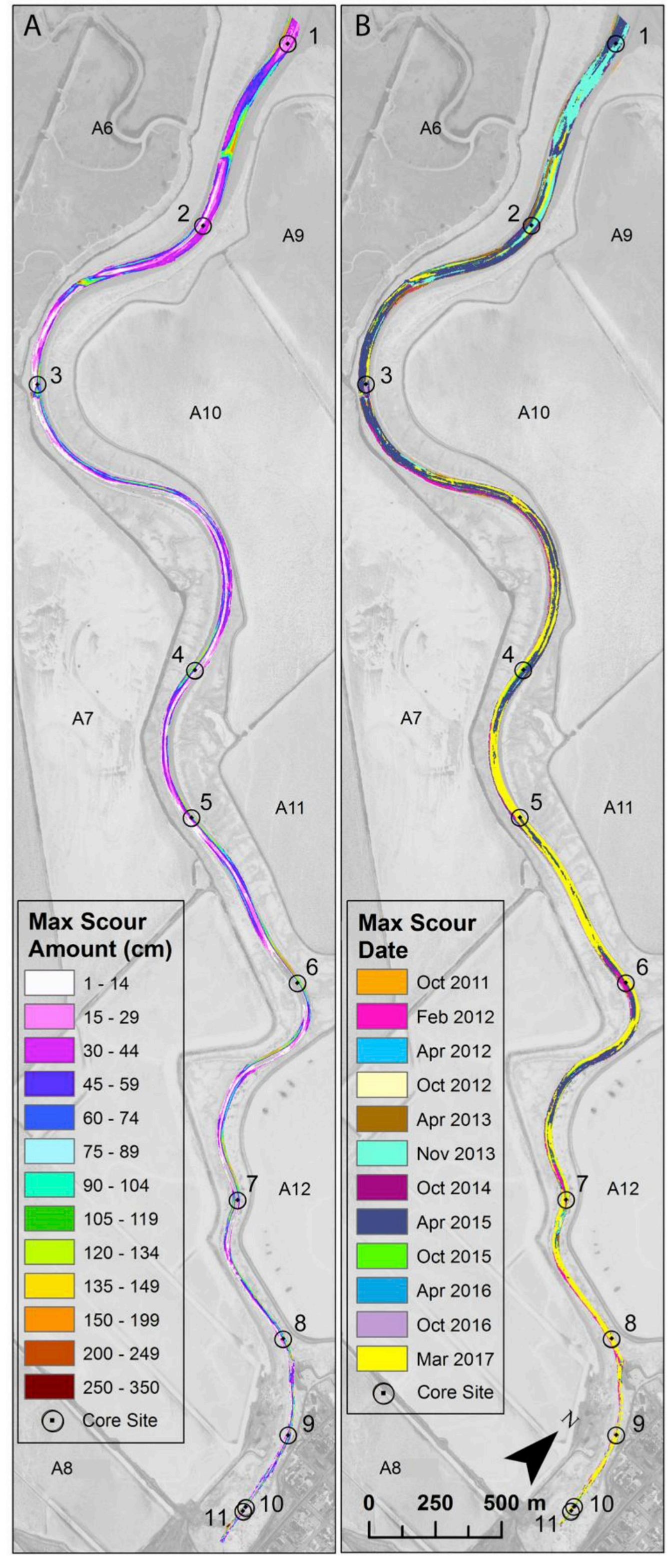

Fig. 5. A: Maximum amount of scour measured throughout all 13 seasonal bathymetric surveys. B: Survey date when the maximum scour depth (left) was reached.

remobilization associated with the sediment scour is shown in Fig. 8. The cumulative volume of sediment eroded throughout the study was greatest in the lower slough (Fig. 8), where THg concentration is lowest. From December 2010–March 2017 an estimated 52 kg (± 3) of THg was remobilized throughout the entire slough and the largest

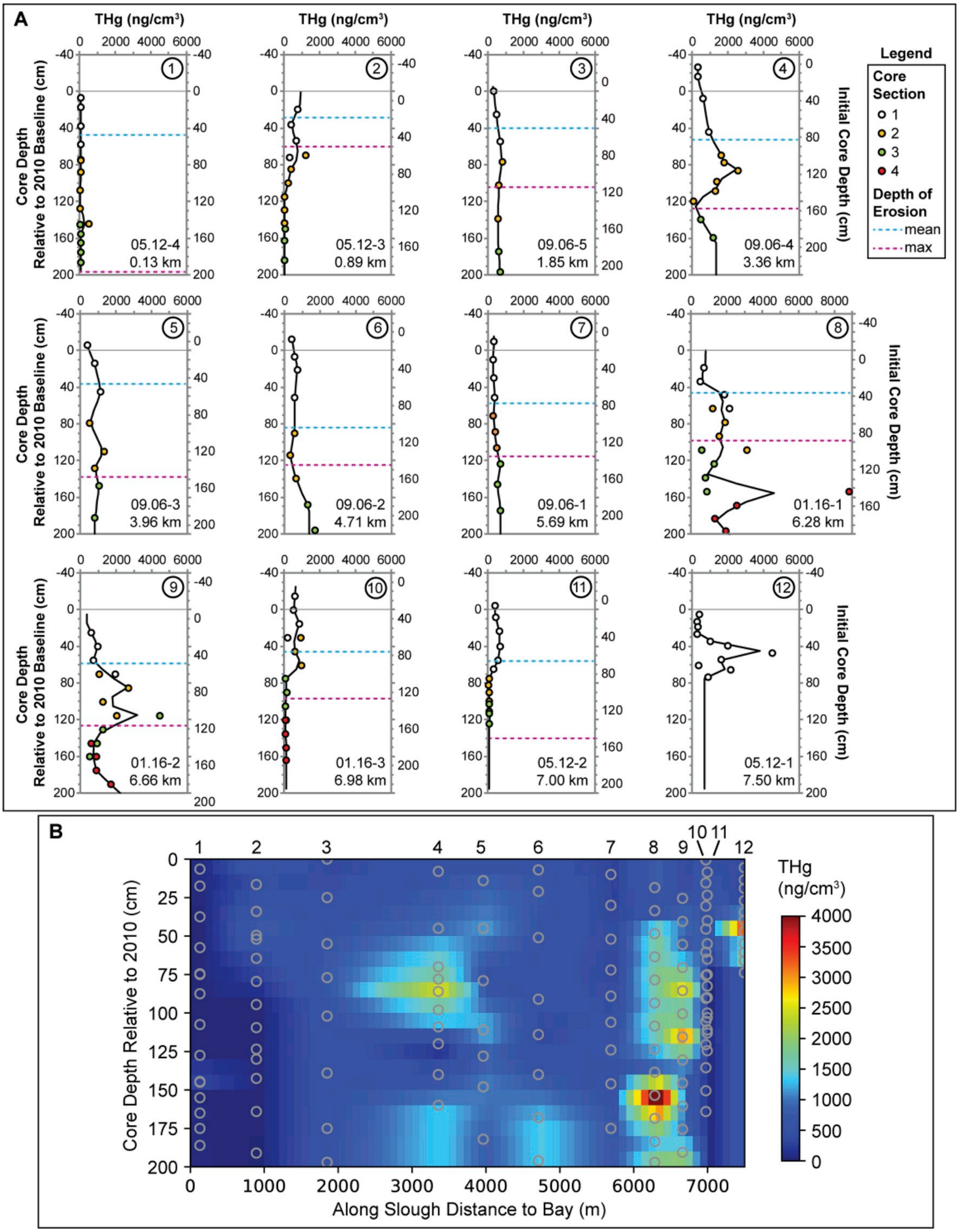

Fig. 6. A: Core data. Sequential core ID in the top right corresponds to locations displayed in Figs. 2 and 3. Core IDs from data reports are shown at the bottom right, the format is collection date (MM.YY) followed by core number. Beneath the core ID is the approximate distance (km) from the mouth of Alviso Slough. The dashed lines represent the mean and maximum depth of scour across a cross-sectional profile taken at each core location. Core 12 (distance 7.50 km) is located up slough of our bathymetric survey extent, thus erosional depths are not displayed. B: Interpolation of THg concentration into 10-cm-thick horizons down-core with a 1-m horizontal resolution. Open circles represent sample measurements.

increases in THg remobilization occurred during the winters of 2012, 2015, and 2017. While the volume of sediment eroded and the mass of THg remobilized generally tracked one another, in the spring of 2015, THg remobilization began to level off in the lower slough while it continued to increase (relative to the amount of sediment scour) in the mid slough (Fig. 8). This trend reflected elevated erosion in the mid slough beginning to reach deeper sediment intervals with higher THg concentrations during October 2014, which continued through March 2017. The average and maximum depths of erosion along a cross-sectional profile at each core location are shown for reference in Fig. 6a. During the winter of 2017, the cumulative amount of THg remobilized in the mid slough exceeded that of the lower slough for the first time since our study began (Fig. 8).

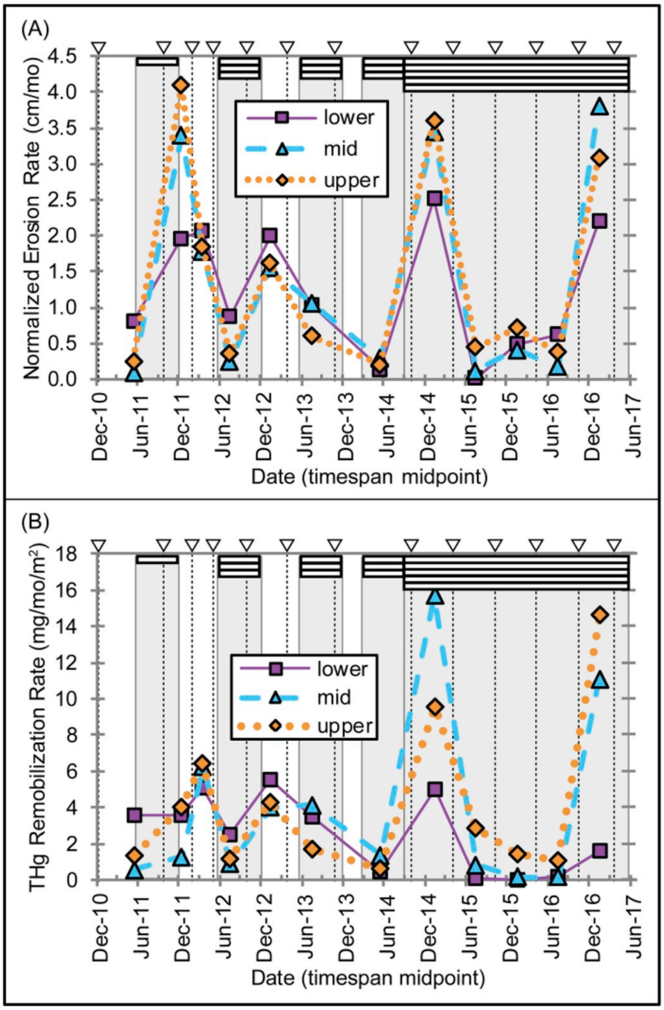

Fig. 7. A: Area-normalized erosion rate by slough reach. B: Area-normalized rate of THg remobilization. Vertical dashed lines represent bathymetric survey dates, the gray shading and rectangles across the X-axis are A8-TCS gate openings (1 box per gate).

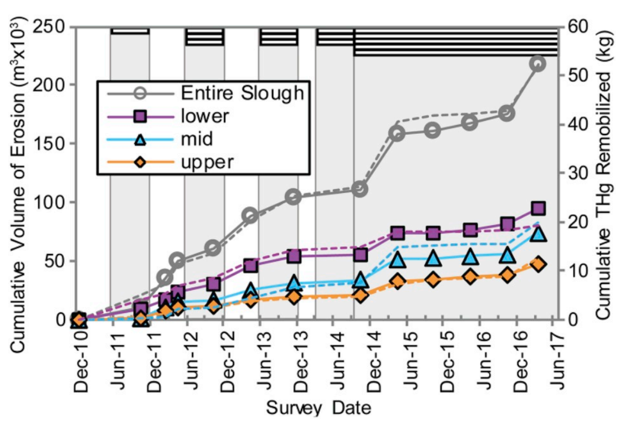

Fig. 8. Cumulative volume of erosion (solid lines) and kilograms of THg remobilized (dashed lines).

5. Discussion

The legacy of mining operations and watershed manipulations remain pronounced in SSFB and provide an additional level of complication to wetland restoration projects. There are both advantages and disadvantages to sediment remobilization within Alviso Slough. Scour remobilizes Hg-contaminated sediments in the slough, which potentially has adverse effects on the ecosystem, but is also a source of sediment to help fill subsided ponds to an elevation that can sustain tidal marsh vegetation, a goal of the restoration project.

Alviso Slough and Pond A6 in particular, exhibit the three characteristics that Williams and Orr (2002) listed as favorable traits for restoration success: (1) a nearly unrestricted tidal exchange, (2) high suspended sediment availability and (3) limited wind-wave induced resuspension. These are undoubtedly characteristics that contributed to the short timespan (approximately 3–5 years) between the Pond A6 breaching in 2010 and when the lower slough became net depositional. This reversal between scour and net sedimentation trends could be indicative of the lower slough beginning to approach a new dynamic equilibrium. In comparison, the Pond A8 complex has experienced restricted tidal exchange through the A8-TCS, is located further up slough where tidal suspended sediment concentration transport is lower, and due to its size and increased fetch, has greater potential for wind-wave induced resuspension. Our measurements showed that the upper slough, as of March 2017, still appeared to be on an erosional trajectory. The maximum depth of scour for much of the mid and upper sloughs occurred in the most recent survey (March 2017) suggesting the mid and upper reaches are still evolving, potentially in direct response to management actions associated with A8-TCS manipulations that continued throughout this study. Until Alviso Slough reaches a new equilibrium, scour will likely continue to remobilize Hg-contaminated sediments.

Our measurements of increased erosion during the winter months and decreased erosion/net deposition during the summer months are consistent with larger patterns of sediment transport documented within SSFB. Periods of high suspended sediment concentration in the spring and summer months measured north of the Dumbarton Bridge (Brand et al., 2010; Lacy et al., 2014) support the common conceptual model that wind-wave resuspension mobilizes sediments north of the Dumbarton Bridge that are then transported to the south (Conomos et al., 1985; Lacy et al., 2014). However, Shellenbarger et al. (2013) did not measure a consistent southern flux through the channel leading to the lower SSFB in the summer months and stressed that the mechanism controlling the timing and direction of net sediment flux through the Dumbarton narrows is not entirely understood. Shellenbarger et al. (2013) hypothesized that salinity gradients (both vertical and longitudinal) over the entire SFB drive gravitational circulation (McCulloch et al., 1970; Walters et al., 1985) and net sediment flux in lower SSFB. These earlier studies, in combination with our broader bathymetric change maps (Figs. S1 and S2), show that seasonal variations in sedimentation persist throughout lower SSFB, and that regional SSFB sediment transport patterns influence sedimentation trends within Alviso Slough.

Over our study period of 6 years, there were three separate peak erosional events that spanned the range of A8-TCS operations and hydrologic conditions. The fact that the three peaks were of similar magnitude, despite varying conditions suggests that a combination of factors influence erosion within Alviso Slough. During the winter of 2012 discharge was low, the rate of erosion was highest in the upper slough and decreased with distance from the A8-TCS. This suggests that the opening of the first A8 gate (1.5 m) in June–December 2011 was at least partially responsible for the increase in erosion. There were no changes to A8-TCS gate configurations between the fall of 2014 and the spring of 2017, yet both winters 2015 and 2017 experienced high net erosion rates, while the intervening winter, 2016, experienced the lowest recorded winter erosion rates throughout our study. Therefore, gate operations were not the only factor controlling scour in the slough and having the A8-TCS open during the winter months did not necessarily or consistently result in enhanced erosion during winter. Rather, the morphology of Alviso Slough has been shaped by a combination of both natural, seasonal variability (in precipitation, winds, and tides) as well as changes in the tidal prism resulting from specific restoration actions.

After 4 years of drought conditions, California experienced record amounts of precipitation in WY 2017 and correspondingly, the Guadalupe River had the highest peak discharge in 19 years and numerous high-flow events. Despite record-high flows, the rate of scour in Alviso Slough was similar to that seen during the winters of 2012 and 2015. One plausible explanation is that scour resulting from increased current velocities during storm events was countered, at least in part, by the massive amount of sediments ($\sim 68 \times 10^6$ kg) delivered over that winter from the upstream watershed (USGS, 2018a). Assuming a sediment bulk density range of 1350–2060 kg/m^3 (range of near-surface samples throughout SSFB; Jones and Jaffe (2013)), this equates to 33×10^3–50×10^3 m^3 of sediment or an amount which would raise the bed elevation of Alviso Slough by approximately 13–20 cm. Of course all of the sediment that passed the Guadalupe gage would not necessarily reach, or stay within Alviso Slough, but some portion likely did. It is also likely that the timing and duration of peak discharge events had an influence on the amount of scour occurring within Alviso Slough. The net impact on scour down slough could be modulated by tidal stage, with current speed and sediment transport down slough amplified on ebb tides and dampened/redirected through the A8-TCS during flood tides (M. Downing-Kunz, pers. comm.). Overall, our measurements support the findings of Shellenbarger et al. (2015) and Achete (2016) who found that episodic winter events can have a large influence on suspended sediment flux for brief periods of time, but the overall net transport patterns are predominantly driven by larger-scale sediment-transport processes.

Although any increase in Hg exposure to the aquatic ecosystem is of concern, our estimate of 52 kg (± 3) of THg over 6.3 years, should also be interpreted in the context of annual loads delivered from the Guadalupe River watershed. Our estimate of 8.2 kg/yr is on the low end of annual estimates of watershed delivery of 7–320 kg/yr (Abu-Saba and Tang, 2000), later refined to 4–30 kg by Thomas et al. (2002). McKee et al. (2017) updated THg flux estimates to incorporate interannual variability and emphasized the importance of intermittent, storm-induced events in transporting larges fluxes of sediment and associated contaminants from upstream watersheds (Whyte and Kirchner, 2000). Based upon 8 years of THg measurements combined with 14 years of suspended sediments loads, McKee at al. (2017) proposed a more refined, climatically adjusted average annual load of 139 kg/yr. Through an intensive, storm-focused sampling regime over 7 days, McKee et al. (2018) estimated that 70 kg of Hg were transported to Alviso Slough over a single storm series in January 2017 and concluded that hundreds of kilograms were likely transported over the winter of 2017. This finding emphasizes the point that high-flow events can have very large impacts and that sources both within estuaries and upstream watersheds must be considered when looking at the potential for contaminant remobilization.

5.1. Limitations of mobilization calculations

There are a number of assumptions and limitations associated with our THg remobilization calculations. First, each core profile is a composite of 3–4 individually collected core segments (approximately 70–80 cm each; see Marvin-DiPasquale and Cox (2007)). Some spatial variability was likely introduced due to the challenges of maintaining an exact sampling position and penetrating the same benthic substrate location with each subsequent sub-core. Second, our interpolation of THg concentration assumes that the THg sampled within the center of the channel is representative of that entire cross-sectional profile (from bank to bank), and that THg varies linearly, between core locations. This layer-cake like approach is undoubtedly an oversimplification as the morphologic behavior of the slough is highly variable, as indicated by changes in depositional and erosional patterns through time, as well as the range of THg concentration present in the cores. Third, for cores where the targeted 2-m penetration depth was not achieved, the deepest THg concentration measured was assigned to the underlying sediments not sampled. There are also a number of reasons why our estimates may be considered a conservative estimate of the total amount of Hg available to the aquatic ecosystem. (1) We only consider sediments above the maximum depth of scour in our remobilization calculations. In reality, any Hg in the shallow sediments just below the maximum depth of scour could be considered part of the new active surface layer exposed to the aquatic environment. (2) Our submerged bathymetric survey system is unable to measure the upper portion of the channel banks closest to the shoreline, thus, we were unable to account for any erosion that occurred above roughly mean tide level. (3) We do not account for Hg associated with incoming sediments deposited within Alviso Slough following our core collections. (4) Lastly, our measurements do not account for continuous sediment reworking within the system. We have quantified where there was a net deposition or erosion of sediment for each given time interval (between consecutive bathymetric surveys), but cannot speak to what happened during intervening times.

6. Conclusions and future work

Restoration projects face a particularly daunting challenge in urbanized estuaries where the remobilization of legacy contaminated-sediments can potentially harm the ecosystem and wildlife they aim to protect. We have presented a new technique for integrating physical measurements of bathymetric scour and THg concentration data within a geographic information system to estimate the amount of THg remobilized within a tidal slough undergoing restoration. Our analysis of 6 years of biannual bathymetric surveys documents the response of Alviso Slough to both natural and human-induced changes. Seasonal surveys captured an overall trend of summertime lows and wintertime highs in erosion rates, which is important to understanding the overall sediment transport patterns. Since restoration began, approximately 52 kg (± 3) of THg was remobilized within the slough. The largest increases in THg remobilization were associated with sediment scour that occurred over winter months and are likely a result of increased discharge during the winter from the Guadalupe River, increased tidal current velocities due to levee breaches and A8-TCS gate operations, as well as larger sediment transport patterns south of the Dumbarton Bridge. After 3–5 years, erosional trends reversed and the lower slough became net depositional, a possible indication that the lower slough is adjusting towards a new equilibrium. In contrast, the middle and upper sloughs were still actively eroding as of our last bathymetric survey in March 2017 and are likely to continue serving as a source for THg remobilization into the future.

Future data collection efforts will be focused on large events (either changes to A8-TCS, the addition of new breaches, or large winter storms) when scour, and thus THg remobilization, are most likely to occur. Additional studies detailing sediment transport pathways would help elucidate the geographic scope and magnitude of ecological impacts resulting from THg remobilization. Methylmercury production is dependent, in part, upon where the remobilized sediments are ultimately deposited, which could be assessed through numerical modeling. To this end, our bathymetric surveys have already been used in the development and validation of sophisticated, process-based numerical models that show promise in tracking sediment-bound mercury and reproducing the morphologic changes we have measured (Achete, 2016; van der Wegen et al., 2018). Through continued refinement of such models we can begin to address crucial questions regarding the ultimate fate of remobilized THg and the long-term evolution of Alviso Slough under various restoration and sea-level rise scenarios. Both the technique presented here and models stemming from this research could be transferred to other study sites to characterize the redistribution of sediment-associated contaminants and inform future restoration projects.

Acknowledgements

Funding for this study was provided by the California Coastal Conservancy, U.S. Environmental Protection Agency, the Resources Legacy Fund, Santa Clara Valley Water District, and the USGS. USGS funding sources included the following programs: Toxic Substances Hydrology, Hydrologic Networks and Analysis, Hydrologic Research and Development, and Coastal and Marine Geology. Any use of trade, firm, or product names is for descriptive purposes only and does not imply endorsement by the U.S. Government. The authors thank the survey crew of the R/V *Parke Snavely*: Mike Boyle, Jackson Currie, Pete Dal Ferro, David Finlayson, Greg Gabel, Jamie Grover, Gerald Hatcher, Rachel Marcuson, Daniel Powers, Jennifer White, and Rob Wyland (all of the USGS Pacific Science Center) who assisted with the bathymetry collection and to Tom Reiss who established base stations for the surveys. Thanks to Jennifer L. Agee, Le H. Kieu, Evangelos Kakouros, and Michelle Arias for the collection, processing, and analyses of mercury samples, to Dave Wahl for help in collecting the 2012 and 2016 cores, and to SeanPaul La Selle for assistance with figures. Thanks to Laura Valoppi and John Bourgeois (SBSPRP) for project coordination and encouragement and to Maureen Downing-Kunz and Trevor O'Neil for insightful sediment transport discussions and watershed data. This manuscript was greatly improved through the thoughtful reviews of Amy East and Christopher Conaway (of the USGS) and three anonymous reviewers.

Appendix A. Supplementary data

Supplementary data to this article can be found online at https://doi.org/10.1016/j.ecss.2019.02.033.

References

Abu-Saba, K.E., Tang, L.W., 2000. Watershed management of mercury in the san Francisco Bay estuary. In: Total Maximum Daily Load Report to U.S. EPA California Regional Water Quality Control Board San Francisco Bay Region, June 30, 2000.

Achete, F.M., 2016. Multiple scales of suspended sediment dynamics in a complex geometry estuary - Dissertation. In: Socio-Economic and Natural Sciences of the Environment. Technology University Delft, EH Leiden, The Netherlands, pp. 138.

Ackerman, J.T., Herzog, M.P., Hartman, C.A., Watts, T., Barr, J., 2014. Waterbird egg mercury concentrations in response to wetland restoration in south San Francisco Bay, California. In: U. S. Geological Survey Open-File Report 2004-1189, pp. 22.

Alpers, C.N., Hunerlach, M.P., May, J.T., Hothem, R.L., 2005. Mercury contamination from historical gold mining in California. In: USGS Fact Sheet 2005-3014 Version 1.1.

Athearn, N.D., Takekawa, J.Y., Jaffe, B., Hattenbach, B.J., Foxgrover, A.C., 2010. Mapping elevations of tidal wetland restoration sites in san Francisco Bay: comparing accuracy of aerial lidar with a singlebeam echosounder. J. Coast Res. 26 (2), 312–319.

Barbier, E.B., Hacker, S.D., Kennedy, C., Koch, E.W., Stier, A.C., Silliman, B.R., 2011. The value of estuarine and coastal ecosystem services. Ecol. Monogr. 81 (2), 169–193.

Barnard, P.L., Foxgrover, A.C., Elias, E.P.L., Erikson, L.H., Hein, J.R., McGann, M., Mizell, K., Rosenbauer, R.J., Swarzenski, P.W., Takesue, R.K., Wong, F.L., Woodrow, D.L., 2013. Integration of bed characteristics, geochemical tracers, current measurements, and numerical modeling for assessing the provenance of beach sand in the San Francisco Bay Coastal System. Mar. Geol. 336, 120–145.

Brand, A., Lacy, J.R., Hsu, K., Hoover, D., Gladding, S., Stacey, M.T., 2010. Wind-enhanced resuspension in the shallow waters of South San Francisco Bay: mechanisms and potential implications for cohesive sediment transport. J. Geophys. Res.: Oceans 115 (C11).

Callaway, J.C., Borgnis, E.L., Turner, R.E., Milan, C.S., 2012. Carbon sequestration and sediment accretion in san Francisco Bay tidal wetlands. Estuar. Coasts 35 (5), 1163–1181.

Callaway, J.C., Schile, L.M., Borgnis, E.L., Busnardo, M., Archbald, G., Duke, R., 2013. Sediment Dynamics and Vegetation Recruitment in Newly Restored Salt Ponds: Final Report for Pond A6 Sediment Study.

Cargill, S.M., Root, D.H., Bailey, E.H., 1980. Resource estimation from historical data: mercury, a test case. J. Int. Assoc. Math. Geol. 12 (5), 489–522.

Chapman, P.M., Wang, F., 2001. Assessing sediment contamination in estuaries. Environ. Toxicol. Chem. 20 (1), 3–22.

Conaway, C.H., Squire, S., Mason, R.P., Flegal, A.R., 2003. Mercury speciation in the san Francisco Bay estuary. Mar. Chem. 80 (2–3), 199–225.

Conaway, C.H., Watson, E.B., Flanders, J.R., Flegal, A.R., 2004. Mercury deposition in a tidal marsh of south San Francisco Bay downstream of the historic New Almaden mining district, California. Mar. Chem. 90 (1), 175–184.

Conomos, T.J., Smith, R.E., Gartner, J.W., 1985. Environmental setting of san Francisco Bay. Hydrobiologia 129 (1), 1–12.

Davis, J.A., Looker, R.E., Yee, D., Marvin-Di Pasquale, M., Grenier, J.L., Austin, C.M., McKee, L.J., Greenfield, B.K., Brodberg, R., Blum, J.D., 2012. Reducing methylmercury accumulation in the food webs of San Francisco Bay and its local watersheds. Environ. Res. 119, 3–26.

Day, J.W., Yáñez-Arancibia, A., Kemp, W.M., 2012. Human impact and management of coastal and estuarine ecosystems. In: Day BCC, J.W., Kemp, W.M., Yáñez-Arancibia, A. (Eds.), Estuarine Ecology.

Eagles-Smith, C.A., Ackerman, J.T., 2014. Mercury bioaccumulation in estuarine wetland fishes: evaluating habitats and risk to coastal wildlife. Environ. Pollut. 193, 147–155.

Eagles-Smith, C.A., Wiener, J.G., Eckley, C.S., Willacker, J.J., Evers, D.C., Marvin-DiPasquale, M., Obrist, D., Fleck, J.A., Aiken, G.R., Lepak, J.M., Jackson, A.K., Webster, J.P., Stewart, A.R., Davis, J.A., Alpers, C.N., Ackerman, J.T., 2016. Mercury in western North America: a synthesis of environmental contamination, fluxes, bioaccumulation, and risk to fish and wildlife. Sci. Total Environ. 568, 1213–1226.

East, A.E., Stevens, A.W., Ritchie, A.C., Barnard, P.L., Campbell-Swarzenski, P., Collins, B.D., Conaway, C.H., 2018. A regime shift in sediment export from a coastal watershed during a record wet winter, California: implications for landscape response to hydroclimatic extremes. Earth Surf. Process. Landforms 43, 2562–2577.

EDAW, Philip Williams & Associates, HT Harvey & Associates, Brown & Caldwell, Geomatrix, 2007. South Bay Salt Pond Restoration Project Final Environmental Impact Statement/Report.

Foxgrover, A., Dartnell, P., Bruce, E.J., Takekawa, J.Y., Athearn, N.D., 2007a. High-resolution bathymetry and topography of South San Francisco Bay, California. In: U. S. Geological Survey Scientific Investigations Map 2987.

Foxgrover, A.C., Finlayson, D.P., Jaffe, B.E., Fregoso, T.A., 2018. Bathymetry and digital elevation models of Coyote creek and Alviso slough, South San Francisco Bay, California. In: U. S. Geological Survey Open-File Report 2011-1315, pp. 24.

Foxgrover, A.C., Jaffe, B.E., Hovis, G.T., Martin, C.A., Hubbard, J.R., Samant, M.R., Sullivan, S.M., 2007b. 2005 hydrographic survey of South San Francisco Bay, California. In: U. S. Geological Survey Open-File Report 2007-1169, pp. 113.

Fulfrost, B., Thomson, D., Archbald, G., Loy, C., Fourt, W., 2012. Habitat Evolution Mapping Project, South Bay Salt Pond Restoration Project Final Report (2009-2011). pp. 91.

Gehrke, G.E., Blum, J.D., Marvin-DiPasquale, M., 2011. Sources of mercury to San Francisco Bay surface sediment as revealed by mercury stable isotopes. Geochem. Cosmochim. Acta 75 (3), 691–705.

Goals Project, 1999. Baylands ecosystem habitat goals. A report of habitat recommendations prepared by the san Francisco Bay area wetlands ecosystem goals project. In: U.S. Environmental Protection Agency, San Francisco. Calif./S.F. Bay Regional Water Quality Control Board, Oakland, Calif.

Grenier, J., Davis, J., 2010. Water Quality in South San Francisco Bay, California: Current Condition and Potential Issues for the South Bay Salt Pond Restoration Project. Springer, New York, NY.

Hornberger, M.I., Luoma, S.N., van Geen, A., Fuller, C., Anima, R., 1999. Historical trends of metals in the sediments of san Francisco Bay, California. Mar. Chem. 64 (1), 39–55.

Ingebritsen, S.E., Jones, D.R., 1999. Santa Clara Valley, California- A case of arrested subsidence. In: In: Galloway, D.L., Jones, D.R., Ingebritsen, S.E. (Eds.), Land Subsidence in the United States, U. S, vol. 1182. Geological Survey Circular, pp. 15–22.

Jaffe, B., Foxgrover, A., 2006. Sediment deposition and erosion in South san Francisco Bay, California from 1956 to 2005. In: U. S. Geological Survey Open-File Report 2006-1287, pp. 24.

Jones, C.A., Jaffe, B.E., 2013. Influence of history and environment on the sediment dynamics of intertidal flats. Mar. Geol. 345, 294–303.

Kirwan, M.L., Megonigal, J.P., 2013. Tidal wetland stability in the face of human impacts and sea-level rise. Nature 504, 53.

Lacy, J.R., Gladding, S., Brand, A., Collignon, A., Stacey, M., 2014. Lateral baroclinic forcing enhances sediment transport from shallows to channel in an estuary. Estuar. Coasts 37 (5), 1058–1077.

Long, E.R., Macdonald, D.D., Smith, S.L., Calder, F.D., 1995. Incidence of adverse biological effects within ranges of chemical concentrations in marine and estuarine sediments. Environ. Manag. 19 (1), 81–97.

Marvin-DiPasquale, M., Cox, M.H., 2007. Legacy mercury in Alviso slough, South San Francisco Bay, California: concentration, speciation and mobility. In: Open-File Report. U.S. Geological Survey, Reston, Virginia, pp. 98.

Marvin-DiPasquale, M.C., Arias, M.R., Agee, J.L., Kieu, L.H., Kakouros, E., Jaffe, B.E., Wahl, D.B., 2018. Mercury speciation and other constituent data from deep sediment cores in Alviso Slough, South San Francisco Bay, California, 2012-16. In: U.S. Geological Survey Data Release, . https://doi.org/10.5066/F7HQ3Z3K.

McCulloch, D.S., Peterson, D.H., Carlson, P.R., Conomos, T.J., 1970. A preliminary study of the effects of water circulation in the san Francisco Bay estuary. In: U. S. Geological Survey Circular 637-A, B. Washington D.C.

McKee, L., Gilbreath, A., Pearce, S., Shimabuku, I., 2018. Guadalupe River mercury concentrations and loads during the large rare january 2017 storm. In: San Francisco Estuary Institute Regional Monitoring Program for Water Quality in San Francisco Bay, Richmond, CA.

McKee, L.J., Bonnema, A., David, N., Davis, J.A., Franz, A., Grace, R., Greenfield, B.K., Gilbreath, A.N., Grosso, C., Heim, W.A., Hunt, J.A., Leatherbarrow, J.E., Lowe, S., Pearce, S.A., Ross, J.R.M., Yee, D., 2017. Long-term variation in concentrations and mass loads in a semi-arid watershed influenced by historic mercury mining and urban pollutant sources. Sci. Total Environ. 605–606, 482–497.

McKee, L.J., Lewicki, M., Schoellhamer, D.H., Ganju, N.K., 2013. Comparison of sediment supply to san Francisco Bay from watersheds draining the Bay area and the central valley of California. Mar. Geol. 345, 47–62.

Miles, A.K., Ricca, M.A., 2010. Temporal and spatial distributions of sediment mercury at

salt pond wetland restoration sites, San Francisco Bay, CA, USA. Sci. Total Environ. 408 (5), 1154–1165.
Nahlik, A.M., Fennessy, M.S., 2016. Carbon storage in US wetlands. Nat. Commun. 7, 13835.
NOAA, 2018. Center for operational oceanographic products and services (CO-OPS) tidal datums. https://tidesandcurrents.noaa.gov/.
Pethick, J.S., 1996. The geomorphology of mudlfat. In: Nordstrom, K.F., Roman, C.T. (Eds.), Estuarine Shores: Evolution, Environment and Human Health. Cambridge University Press, Cambridge, UK, pp. 41–62.
Poland, J.F., Ireland, R.L., 1988. Land subsidence in the Santa Clara Valley, California, as of 1982. In: U.S. Geological Survey Professional Paper 497-F, pp. 61.
Ramsar Convention, 2018. Ramsar Convention on Wetlands. Global Wetland Outlook: State of the World's Wetlands and Their Services to People. in, Gland, Switzerland.
Rodríguez, J.F., Saco, P.M., Sandi, S., Saintilan, N., Riccardi, G., 2017. Potential increase in coastal wetland vulnerability to sea-level rise suggested by considering hydrodynamic attenuation effects. Nat. Commun. 8, 16094.
SBSPRP, 2018. South Bay salt pond restoration project website. http://www.southbayrestoration.org/science/.
Schwarzbach, S.E., Albertson, J.D., Thomas, C.M., 2006. Effects of predation, flooding, and contamination on reproductive success of California. Clapper Rails in San Francisco Bay The Auk 123 (1), 45–60.
SFEI, 2018. Resilient landscape vision for the calabazas creek, san tomas aquino creek, and pond A8 area: bayland-creek reconnection opportunites. In: A SFEI-ASC Resilient Landscape Program Report Developed in Cooperation with the Healthy Watersheds, Resilient Baylands Design Advisory Team, Santa Clara Valley Water District, and South Bay Salt Ponds Restoration Project, Publication #870. San Francisco Estuary Institute Aquatic Science Center, San Francisco Estuary Institute Aquatic Science Center, Richmond, CA.
Shellenbarger, G.G., Downing-Kunz, M.A., Schoellhamer, D.H., 2015. Suspended-sediment dynamics in the tidal reach of a San Francisco Bay tributary. Ocean Dynam. 65 (11), 1477–1488.
Shellenbarger, G.G., Wright, S.A., Schoellhamer, D.H., 2013. A sediment budget for the southern reach in San Francisco Bay, CA: implications for habitat restoration. Mar. Geol. 345, 281–293.
Swain, D.L., Langenbrunner, B., Neelin, J.D., Hall, A., 2018. Increasing precipitation volatility in twenty-first-century California. Nat. Clim. Change 8 (5), 427–433.
Thomas, M.A., Conway, C.H., Steding, D.J., Marvin-Di Pasquale, M., Abu-Saba, K.E., Flegal, A.R., 2002. Mercury contamination from historic mining in water and sediment, Guadalupe River and san Francisco Bay, California. Geochem. Explor. Environ. Anal. 2 (3), 211–217.
USGS, 2018a. Discharge and suspended sediment records 2002-2018 from gaging station 1169025, Guadalupe River at highway 101, san Jose, California. https://waterdata.usgs.gov/nwis/uv?site_no=11169025.
USGS, 2018b. Peak streamflow records 1930-2003 from gaging station 1169000, Guadalupe River, san Jose, California. https://nwis.waterdata.usgs.gov/ca/nwis/peak?site_no=11169000.
van der Wegen, M., Reyns, J., Jafffe, B., Foxgrover, A., 2018. Modeling morphodynamic development in the Alviso slough system, South San Francisco Bay. In: Report for the Santa Clara Valley Water District.
Walters, R.A., Cheng, R.T., Conomos, T.J., 1985. Time scales of circulation and mixing processes of San Francisco Bay waters. Hydrobiologia 129 (1), 13–36.
Watson, E.B., 2004. Changing elevation, accretion, and tidal marsh plant assemblages in a South San Francisco Bay tidal marsh. Estuaries 27 (4), 684–698.
Whyte, D.C., Kirchner, J.W., 2000. Assessing water quality impacts and cleanup effectiveness in streams dominated by episodic mercury discharges. Sci. Total Environ. 260 (1), 1–9.
Williams, P.B., Orr, M.K., 2002. Physical evolution of restored breached levee salt marshes in the san Francisco Bay estuary. Restor. Ecol. 10 (3), 527–542.
Wright, G., Gustin, M.S., Weiss-Penzias, P., Miller, M.B., 2014. Investigation of mercury deposition and potential sources at six sites from the Pacific Coast to the Great Basin. USA. Sci. Total Environ. 470–471, 1099–1113.